The Competitive Interaction of Actin and PIP_2 with Actophorin Is Based on Overlapping Target Sites: Design of a Gain-of-Function Mutant†

Marleen Van Troys, Daisy Dewitte, Jean-Luc Verschelde, Marc Goethals, Joël Vandekerckhove, and Christophe Ampe*

Department of Biochemistry, Ghent University, and Flanders Interuniversity Institute for Biotechnology (VIB), Ledeganckstraat 35, 9000 Gent, Belgium

Received April 11, 2000; Revised Manuscript Received July 31, 2000

ABSTRACT: We studied the effect of mutations in an α-helical region of actophorin (residues 91−108) on F-actin and PIP_2 binding. As in cofilin, residues in the NH_2-terminal half of this region are involved in F-actin binding. We show here also that basic residues in the COOH-terminal half of the region participate in this interaction whereby we extend the previously defined actin binding interface [Lappalainen, P., et al. (1997) *EMBO J. 16*, 5520−5530]. In addition, we demonstrate that some of the lysines in this α-helical region in actophorin are implicated in PIP_2 binding. This indicates that the binding sites of F-actin and PIP_2 on actophorin overlap, explaining the mutually exclusive binding of these ligands. The Ca^{2+}-dependent F-actin binding of a number of actophorin mutants (carrying a lysine to glutamic acid substitution at the COOH-terminal positions of the actin binding helical region) may mimic the behavior of members of the gelsolin family. In addition, we show that PIP_2 binding, but not actin binding, of actophorin is strongly enhanced by a point mutation that leads to a reinforcement of the positive electrostatic potential of the studied α-helical region.

The ADF[1]/cofilin family of actin binding proteins is ubiquitously present in eukaryotic species (*1*). These proteins are required for the high turnover of the actin cytoskeleton (*2*−*4*) which forms the basis of numerous essential processes in vivo. The yeast cofilin null mutant is not viable (*5*, *6*), and various representatives of the family are shown to be implicated in cytokinesis (*7*, *8*), cellular motility, and shape changes (*9*, *10*). ADF/cofilins interact with both monomeric and filamentous actin (*11*, *12*) and bring about an acceleration of the actin depolymerization−polymerization process. This is achieved either by severing (*12*−*14*) or by increasing the rate of dissociation of actin subunits from the pointed end of actin filaments (*15*, *16*). Consequently, by feeding the monomer pool, they also increase the rate of association at the barbed end, resulting in an enhanced filament turnover (*15*). Accordingly, the rate of overall actin depolymerization in yeast cells expressing a mutated cofilin is shown to be decreased compared to the wild-type situation (*2*).

Three factors have been described that regulate and affect the action of cofilin on actin filaments. First, LIM kinase, acting downstream of Rho-family GTPases (*17*, *18*), phosphorylates cofilin on an NH_2-terminal serine residue, resulting in the loss of actin binding (*19*−*22*). Second, actin interacting protein 1 (Aip-1) forms a ternary complex with actin and cofilin, cooperating with the latter to disassemble actin filaments (*23*−*25*). Last, polyphosphoinositides interact with cofilin in vitro and inhibit its binding to actin (*26*, *27*). Evidence for the in vivo relevance of this activity was indirectly presented in a microinjection study of cofilin and phosphatidylinositide 4,5-bisphosphate (PIP_2) in muscle cells by Nagaoka et al. (*28*).

The degree of sequence similarity between members of the ADF/cofilin family is extremely high in an α-helical region (residues 112−128 in porcine cofilin and residues 91−108 in actophorin) (*29*) that has a structural irregularity in its central region, leading to a kinked α-helix in cofilin or a helix−turn−helix structure in actophorin (*30*−*32*). This region has been implicated in actin binding (*1*, *33*). In this amino acid stretch, actophorin, the cofilin homologue from *Acanthamoeba castellanii* (*27*, *34*), only differs at five residues from porcine cofilin (two of which are conservative substitutions). Two highly conserved basic residues in the extreme NH_2-terminal part of this helical region were shown to be involved in the contact of cofilin with actin (*35*, *36*). Moriyama et al. (*35*) demonstrated that the first of these NH_2-terminal lysines is also implicated in PIP_2 binding. However, the role of other residues in PIP_2 binding is unexplored.

In this report, we present a mutational analysis of this α-helical region. We design variants of the corresponding cofilin peptide (residues 102−131), create mutants of acto-

† This work was supported by the Human Capital and Mobility Program of the European Community CHRX 0430, Grant GOA-91/96-3 to J.V., a grant from the "Koning Boudewijn Stichting" to C.A., FWO Grants G006096 to J.V. and G004497 to C.A., and a grant from the Interuniversity Attraction Poles (IUAP 0.34) to J.V. C.A. is a research associate and M.V.T. a postdoctoral fellow of the Fund for Scientific Research Flanders FWO-Vlaanderen.

* To whom correspondence should be addressed: Department of Biochemistry, Faculty of Medicine, Ghent University, Ledeganckstraat 35, B-9000 Gent, Belgium. Telephone: 32 9 264 53 06. Fax: 32 9 264 53 37. E-mail: Champ@gengenp.rug.ac.be.

[1] Abbreviations: ADF, actin depolymerizing factor; EDC, 1-ethyl-3-[3-(dimethylamino)propyl]carbodiimide; P1−P5, cofilin peptides; PIP_2, phosphatidylinositol 4,5-bisphosphate; SDS−PAGE, sodium dodecyl sulfate−polyacrylamide gel electrophoresis; WT, wild type.

10.1021/bi000816c CCC: $19.00
Published on Web 09/14/2000

phorin, and examine the impact of the mutations on both F-actin and PIP_2 binding. Our analysis reveals also that the COOH-terminal lysines of the α-helical region are involved in both activities, but more importantly shows a clear, albeit partial, overlap between the two binding sites. Surprisingly, the reduced actin binding of a number of actophorin mutants can be partially restored in the presence of Ca^{2+}. In view of the structural and functional similarity between the cofilin and gelsolin family (*29*, *30*, *33*), this provides insight into the mechanism of Ca^{2+} dependency of actin binding by segments of gelsolin and related proteins. In addition, we designed an actophorin gain-of-function mutant with regard to PIP_2 binding that may prove to be useful in further studies on the complex regulation of cofilins in vivo.

EXPERIMENTAL PROCEDURES

Peptides and Proteins

Cofilin wild type (WT) and mutant peptides were chemically synthesized on a model 431A peptide synthesizer (Applied Biosystems Inc., Foster City, CA). We checked their purity and mass as described in ref *37*. The peptides were labeled with ^{14}C on methionine 115 using [^{14}C]-methyliodide (Dupont), according to the method of ref *38*. After labeling, the peptides were purified via reversed phase high-pressure liquid chromatography, lyophilized, and dissolved in 10 mM phosphate buffer (pH 7.5). The peptide concentration was determined by following the method of Vancompernolle et al. (*39*). A competition assay between labeled and nonlabeled WT peptide proved that both bind actin with the same affinity (data not shown).

Ca−ATP−G-actin was prepared from rabbit skeletal muscle as described by Spudich and Watt (*40*) and further purified over a Sephadex G-200 gel filtration column in G-buffer [5 mM Tris-HCl (pH 7.7), 0.1 mM $CaCl_2$, 0.2 mM ATP, 0.2 mM DTT, and 0.01% NaN_3]. The actin was labeled with *N*-pyrenyliodoacetamide on Cys374 (*41*).

WT actophorin was prepared recombinantly in *Escherichia coli* using a T7 expression vector carrying the actophorin cDNA, which was generously provided by T. Pollard. To introduce mutations into the actophorin gene, we used the polymerase chain reaction-based overlap extension mutagenesis approach (*42*). Mutant cDNAs were cloned either as *Nde*I−*Bam*HI or as *Nco*I−*Bam*HI fragments in the pET3a or pET11d expression vector, respectively (Promega). In the latter case, the mutant actophorins carry an additional alanine following the NH_2-terminal methionine. All DNA constructions were sequenced using an ALF EXPRESS DNA Sequenator (Pharmacia Biotech) or an ABI Prism 377 Automated Sequencer (Applied Biosystems). We purified actophorin (WT or mutants) as described by Quirck et al. (*27*). As a final concentration step, the proteins were dialyzed against 20% polyethylene glycol (MW_{av} = 20000) in the appropriate buffer solution.

The unfolding profiles of the WT and mutant actophorins as a function of urea concentration were recorded by measuring the intrinsic tryptophan fluorescence emission spectrum. The proteins were diluted to 10 or 20 μM in urea, buffered with 20 mM Tris-HCl (pH 8.0). We performed the measurements on an F-4500 fluorimeter (Hitachi) (excitation at 295 nm and emission at 327 nm) at room temperature.

Actin Binding Assays

Chemical Cross-Linking Experiments. Cross-linking using EDC of the cofilin peptides or actophorin proteins to prepolymerized actin (10 μM) was performed as described by Van Troys et al. (*33*). Spinning these samples at high speed confirms that cofilin peptides and actophorins are cross-linked to actin filaments (not shown). The degree of cross-linking by the labeled cofilin peptides was quantified from SDS gels using a PhosphorImager (Molecular Dynamics) and the ImageQuant software package. Both the WT and variant peptides had a specific activity of 8000 cpm/nmol of peptide, allowing easy comparison of the yield of cross-linking. We used densitometry of SDS gels to determine the WT or mutant actophorin concentrations at which maximal cross-linking is reached.

Cosedimentation Assay. To study the cosedimentation of actophorin (WT or mutants) with actin filaments (actin concentration of 10 μM), we followed the same procedure described by Van Troys et al. (*33*). After centrifugation, the supernatant and resuspended pellet were analyzed on SDS gels followed by Coomassie staining. We used densitometry to quantify the results.

Depolymerization Assay. Barbed end-capped actin filaments were prepared by overnight incubation on ice of polymerized actin (8 μM, 25% pyrene labeled) with gelsolin (40 nM, gelsolin:actin molar ratio of 1:50). These were diluted in G-buffer to a final concentration of 0.4 μM in the absence or presence of WT or mutant actophorin at the concentrations indicated in the legend of Figure 3. The fluorescence decrease was recorded over the course of 8 min on an F-4500 fluorimeter (Hitachi) (excitation at 365 nm and emission at 388 nm). The G-buffer was supplemented with either $CaCl_2$ (0.1−1 mM) or EGTA (1 mM).

PIP_2 Binding Assays

Gel Filtration Chromatography. We incubated WT or mutant actophorin with increasing concentrations of PIP_2 (Sigma) micelles in 25 mM Tris-HCl, 50 mM KCl, 0.2 mM DTT, and 0.2 mM EGTA (pH 7.5) for 20 min at 22 °C. Subsequently, the samples were loaded on a Superdex 75 gel filtration column (75PC3.2/30, Pharmacia), equilibrated in the same buffer, on a Smart fast protein liquid chromatography system (Pharmacia). PIP_2 micelles and actophorin bound to micelles elute in the column flow through, and free actophorin is retarded on the column. The amount of free protein (and based here upon the amount of bound protein) was obtained by integration of the absorption peak (A_{280}). We used 5 μM (or 20 μM for Figure 4B) WT or mutant actophorin; the PIP_2 concentrations ranged from 0 to 125 μM (from 0 to 350 μM for Figure 4B).

Via Microfiltration. Microfiltration assays were performed as described by Lambrechts et al. (*43*). In brief, 5 μM WT or mutant actophorin was incubated for 30 min on ice with PIP_2 micelles (0−450 μM PIP_2) prior to spinning for 1 min at 4000*g* in a microfiltration device with a molecular weight cutoff of 30 000 (Millipore). PIP_2 micelles and actophorin that is bound to micelles remain in the retentate; a fraction of the filtrate containing the free protein was analyzed on SDS−PAGE.

F-Actin vs PIP_2 Competition Assay

We incubated F-actin (15 μM), which was polymerized starting from Mg−ATP−G-actin using 100 mM KCl, with WT or D102K actophorin (15 μM) in 5 mM Tris-HCl (pH 7.7), 0.2 mM ATP, 0.2 mM DTT, and 40 mM KCl prior to adding increasing amounts of micellar PIP_2 (PIP_2 concentration ranging from 0 to 300 μM). The actin-bound actophorin was visualized by SDS−PAGE analysis of the pellets after high-speed sedimentation (10 min at 100000*g*, Beckman Airfuge). Free and PIP_2 micelle-bound actophorin remain in the supernatant. F-Actin-bound actophorin was quantified using densitometry (TotalLab, Phoretix International).

Calculation of the Electrostatic Potential of Actophorin and Actophorin Mutant D102K

The electrostatic potentials of the proteins were calculated using the DELPHI software (Molecular Simulations) with default setup parameters using a grid that contains the molecule. For each protein, two contours are created. One contour (in blue) connects all grid points that have a potential value of 2.5 kT/e, and a second contour (in red) connects all grid points that have a potential of −2.5 kT/e. We analyzed the results using the INSIGHT II package.

RESULTS

Analysis of Actin Binding by a Set of Variant Cofilin Actin Binding Peptide Mimetics. As a pilot experiment, a set of synthetic peptides corresponding to the cofilin sequence ranging from amino acid 102 to 131 (with amino acids 112−128 forming the α-helical region of interest) and carrying lysine to glutamic acid exchanges in various combinations was synthesized. The ability of the peptides to form α-helices in 60% 2,2,2-trifluoroethanol was compared to that of the wild type (WT) peptide (P1, Table 1) using circular dichroism measurements (not shown). Only those peptides (P2−P5, Table 1) that exhibited a WT or a quasi-WT spectrum were further studied. The actin binding of each peptide was assayed in a cross-linking experiment in which the peptide was added to polymerized actin and treated with the zero-length cross-linker EDC. Peptides were radiolabeled to allow a quantification of the yield of cross-linking as a function of peptide concentration (Figure 1). P1, representing the WT actin binding α-helical region, reaches a plateau value of cross-linking (set at 100%) at about 50 μM peptide. For the variant peptides, in which lysine residues at either the start (P2, residues 92 and 94) or the end (P3, residues 105−107; P4, residue 105) of the α-helical region were substituted, much higher concentrations are needed to obtain a high yield of cross-linking. The effect of combining charge reversals in the NH_2- and COOH-terminal part of the α-helical region (P5, KK114,125EE) proved to be even more dramatic. Taken together, these results clearly indicate that basic residues at either end of this α-helical region in cofilin are implicated in the contact with actin.

Generation and Stability of Actophorin Mutants. As a followup to these peptide data, we set out to study the effect of mutations in this α-helical region in a native protein background, here actophorin, the cofilin homologue from *A. castellanii* (*27*). Mutants having either a single (e.g., K92E), a double (e.g., KD101,102AA), or a triple amino acid substitution (KKK105,106,107EEE) were created (Table 1). In analogy to WT, our actophorin mutants were produced in high amounts as soluble protein in *E. coli*, and we were able to purify them using the same purification procedure (*27*). All mutants were essentially pure as judged by SDS−PAGE of 2.5 μg of the purified material (not shown).

Given our experience with the mutant peptide mimetics, we ensured that the actophorin mutants have a stable conformation under the conditions used in our actin binding assays. Therefore, we assessed unfolding as a function of increasing urea concentrations. Most mutants start unfolding

Table 1: Sequences of WT and Variant Cofilin Peptides and Mutant Positons (underlined) in Actophorin and Stability of the Actophorin Mutants

cofilin peptides (residues 102-131)		
P1(WT)	IFWAPECAPLKSKMIYASSKDAIKKKLTG	
P2	IFWAPECAPLESEMIYASSKDAIKKKLTG	
P3	IFWAPECAPLKSKMIYASSKDAIEEELTG	
P4	IFWAPECAPLKSKMIYASSKDAIEKKLTG	
P5	IFWAPECAPLKSEMIYASSKDAIEKKLTG	
actophorin (residues 91-108)		*urea concentration at start denaturation*
WT	IKSKMMYTSTKDSIKKKL	3M
K92E	IESKMMYTSTKDSIKKKL	3M
K94E	IKSEMMYTSTKDSIKKKL	0.75M
D102K	IKSKMMYTSTKKSIKKKL	1M
K105E	IKSKMMYTSTKDSIEKKL	1M
K106E	IKSKMMYTSTKDSIKEKL	2M
K107E	IKSKMMYTSTKDSIKKEL	0.5M
KK92,94EE	IESEMMYTSTKDSIKKKL	not stable
KD101,102AA	IKSKMMYTSTAASIKKKL	3M
KD101,102DK	IKSKMMYTSTDKSIKKKL	0.5M
KK105,106EE	IKSKMMYTSTKDSIEEKL	1M
KK105,107EE	IKSKMMYTSTKDSIEKEL	1M
KK106,107EE	IKSKMMYTSTKDSIKEEL	1.5M
KKK105,106,107EEE	IKSKMMYTSTKDSIEEEL	1.5M

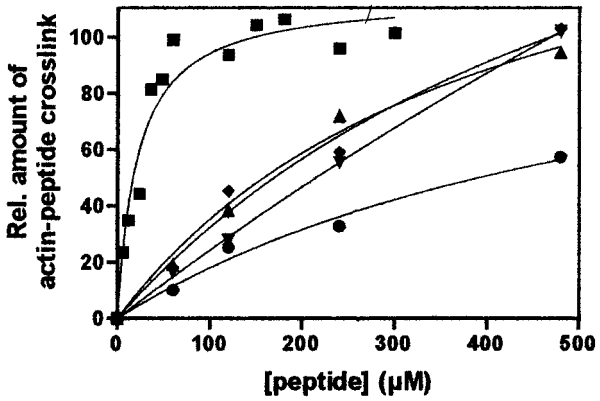

FIGURE 1: Chemical cross-linking of cofilin peptides (WT and variants) to F-actin. Increasing concentrations of radiolabeled peptides (for nomenclature, see Table 1) were chemically cross-linked to 12 μM prepolymerized actin and analyzed by SDS−PAGE. We quantified the gels using a PhosphorImager system. The graph shows the relative amount of cross-linking as a function of peptide concentration: WT P1 (■), P2 (▲), P3 (▼), P4 (◆), and P5 (●).

at lower urea concentrations than WT (Table 1). This is possibly due to small local differences that occur upon introduction of an oppositely charged residue, disrupting, among other structures, internal salt bridges.[2] We experienced difficulties purifying mutants K94E, KK92,94EE, K107E, and KD101,102DK, suggesting the introduced mutation affects the stability of these proteins. Although only very small amounts of urea are necessary to induce unfolding of mutants K94E, K107E, and KD101,102DK, their denaturation profiles start with a plateau value.[2] Thus, all but one mutant (KK92,94EE) adopt a stable conformation at 0 M urea and, hence, under the conditions used in the assays described below. Mutant KK92,94EE was not further investigated.

Charge Changes at Both Ends of the α-Helical Region Affect Actin Binding by Actophorin. We examined the actophorin mutants for their ability to interact with actin under physiological salt conditions. As for the cofilin peptides, their capacity to cross-link to F-actin was compared to that of WT actophorin. Adding 15 μM WT actophorin to 10 μM prepolymerized actin results in the maximal formation of the cross-linked actin−actophorin complex (50% relative to the total amount of actin). This and the cross-linking data for one actophorin mutant (KK105,107EE) are shown in Figure 2A. For all mutants, the data are summarized in Table 2. In a second binding assay, we analyzed the amount of WT or mutant actophorin that associates with F-actin. The protein composition of the pellets obtained after high-speed sedimentation of WT and one mutant (K107E) is shown in Figure 2B; for all mutants, the data are given in Table 2.

Consistent with our cofilin peptide data, lysine to glutamic acid substitutions at positions 92, 94, and 105−107 in actophorin lead to a reduction in the F-actin binding capacity of actophorin. The change of K94 in the NH_2-terminal α-helix has by far the most dramatic effect, followed by substitution of K92, K107, and K106. K105 is least affected. This again indicates that both ends of this α-helical stretch are implicated in the contact with F-actin.

Both assays were also used to test the double and triple mutants (Table 2). Substitution of either K105 or K106 in combination with K107 does not strongly enhance the already substantial phenotype of the latter mutation. Likewise, combining the change of lysines 105 and 106 resembles the K106E mutation in the cross-linking assay, although the sedimentation assay shows that binding is more strongly affected than for either single mutation. The triple mutant KKK105,106,107EEE does not interact or only very weakly interacts with F-actin at the highest concentration that was tested.

For some mutants, we observe minor differences in the binding data obtained with each of the two assays that were used. The formation of a cross-linked actin−actophorin complex depends on the permanent fixation of an established electrostatic contact. Consequently, the cross-linking capacity of a number of actophorin charge reversal mutants may be more severely affected than their ability to cosediment with F-actin (e.g., for K92E, D102K, and K106E), suggesting that these may be involved in salt bridges in the actin−actophorin interface. Alternatively, these mutations may influence the cross-linking capacity of a neighboring residue.

[2] J.-L. Verschelde et al., unpublished results.

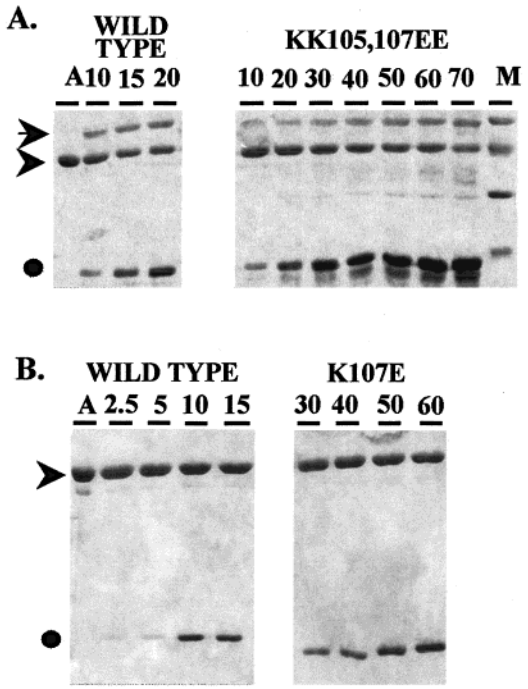

FIGURE 2: Binding of actophorin mutants to F-actin. (A) SDS−PAGE analysis of the chemical cross-linking of actophorin WT and mutant KK105,107EE to prepolymerized actin (10 μM). The actophorin concentration is indicated in micromolar above each lane. A denotes actin in the absence of actophorin. Actin, the cross-linked actin−actophorin complex, and free actophorin are indicated by an arrowhead, arrow, and closed circle, respectively. Molecular mass markers of 20, 30, 43, and 67 kDa are shown. (B) SDS analysis of resuspended pellets of a cosedimentation experiment of actophorin WT and mutant K107E (concentration in micromolar above each lane) with F-actin (10 μM) (actin, arrowhead; actophorin, closed circle). The lane headed A contained only actin. All mutants were tested using these two assays; the quantified data are shown in Table 2.

Table 2: Binding of WT and Mutant Actophorin to F-Actin[a]

	maximal cross-linking (50%)	saturation of cosedimentation
WT	15 μM	10 μM
K92E	ns[b]	50−60 μM
K94E	nc[c]	ns[d]
D102K	15 μM	20−25 μM
K105E	20−30 μM	20 μM
K106E	70 μM	15 μM
K107E	75 μM	55 μM
KD101,102AA	15−20 μM	15−20 μM
KD101,102DK	30 μM	50 μM
KK105,106EE	55−60 μM	100 μM
KK105,107EE	65−70 μM	60 μM
KK106,107EE	75 μM	75 μM
KKK105,106,107EEE	nc[c]	70−80 μM

[a] Actin concentration of 10 μM. ns, no saturation. [b] Fifteen percent cross-linking at 75 μM. [c] No cross-linking at 90 μM. [d] Five percent cosedimenting at 50 μM.

Ca^{2+} Partially Restores the Activity of Actophorin Mutated in the COOH-Terminal Half of the α-Helical Region. The in vitro actin interaction of WT actophorin and of other members of the cofilin/ADF family is independent of Ca^{2+}. Because of a number of arguments, including the high degree of structural similarity (*30*) and the functional analogy (*33*) of these proteins to segment 2 of gelsolin, in addition to the differential Ca^{2+} dependence of members of the gelsolin family in their F-actin interaction (*44*, *45*) (see also the

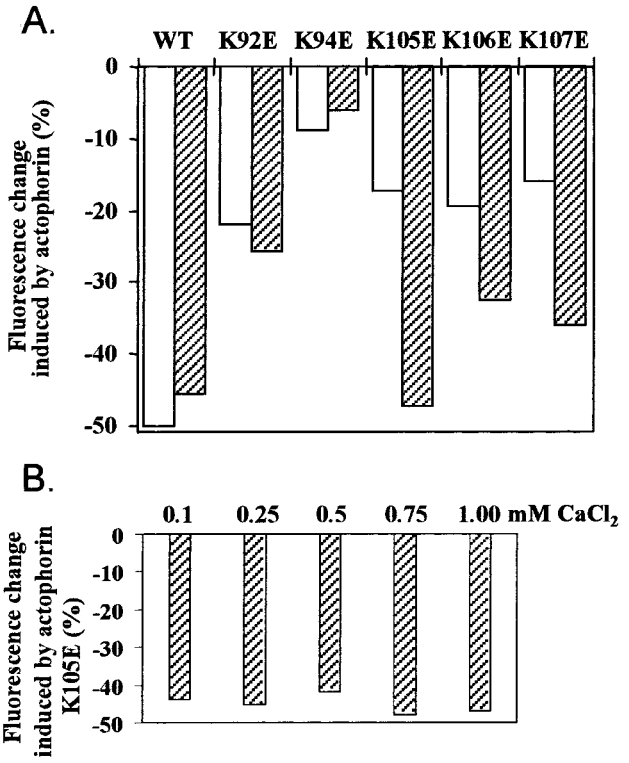

FIGURE 3: Ca^{2+} dependency of actin binding of selected actophorin mutants. (A) Effect of Ca^{2+} on the fluorescence decrease observed 8 min after dilution of F-actin (25% pyrene-labeled, capped at barbed end) to 0.4 μM in G-buffer supplemented with either 1 mM EGTA (white bars) or $CaCl_2$ (hatched bars), and containing WT, K92E, K94E, K105E, K106E, or K107E at 0.6, 4.8, 1.2, 1.2, 2.4, or 3 μM, respectively. The *Y*-axis is the decrease in fluorescence induced by actophorin (WT or mutant) corrected for the decrease already observed in control samples with only actin. This change is expressed as a percentage of the start fluorescence and proportional to $100(F_c - F_a)/F_0$, with F_0 being the initial fluorescence and F_c and F_a being the fluorescence decrease 8 min after dilution of the control sample and the sample containing actophorin, respectively. (B) The fluorescence decrease induced by mutant K105E using the same assay as described for panel A is shown as a function of $CaCl_2$ concentration.

Discussion), we analyzed whether Ca^{2+} could alleviate the decrease in F-actin binding capacity of our actophorin mutants. We used an assay in which barbed end-capped, pyrene-labeled actin filaments are induced to depolymerize by dilution. Actophorin (and other family members) enhances the rate of monomers dissociating from the pointed end but in addition quenches the fluorescence of the pyrene label upon binding to the actin filament (*12*, *15*). This combined effect of actophorin binding, thereby promoting depolymerization, results in a strong decrease in fluorescence (compared to a control sample containing only actin). Of interest to us is the fact that for WT actophorin the resulting reduction in the magnitude of the fluorescent signal is approximately the same in the presence or absence of $CaCl_2$ (Figure 3A). For the mutants carrying changes in the COOH-terminal half of the α-helical region, the results in EGTA confirm our binding data presented above. Note that although the mutants are used at higher concentrations than WT (see the legend of Figure 3A), they display less than half of the WT activity. Upon comparison of the fluorescence decrease induced by the mutants in either $CaCl_2$ or EGTA, it is evident that in the presence of Ca^{2+} the effect on fluorescence is stronger for K105E, K106E, and K107E. Indeed, for these mutants, the resulting change in fluorescence in $CaCl_2$ is about 1.5−3 times higher than in EGTA (Figure 3A). This stronger effect in $CaCl_2$ versus EGTA remained constant within a range of 0.1−1 mM $CaCl_2$ as shown for K105E in Figure 3B. The Ca^{2+} dependency of the fluorescence decrease suggests that mutants K105E, K106E, and K107E bind more strongly to actin in the presence of Ca^{2+} than in its absence. In contrast, for WT and for mutants K92E and K94E, the fluorescence decrease hardly differs with or without $CaCl_2$ (Figure 3A), suggesting that the differential signal observed for mutants K105E, K106E, and K107E is indeed due to a different binding capacity and not to a different quenching factor per molecule bound in $CaCl_2$ versus EGTA.

Taken together, these results suggest that the effect of charge changes at specific positions in the COOH-terminal part of the actin binding α-helical region can be partly counteracted by Ca^{2+} ions.

Residues in the Actin Binding α-Helical Region Also Contact PIP_2. Actophorin binds to the phosphoinositide PIP_2 in a concentration-dependent manner (*27*), and Yonezawa et al. (*26*) demonstrated that the binding of cofilin to PIP_2 and actin is mutually exclusive. Consequently, we were interested in determining the effect of the mutations, introduced into the actin binding region, on PIP_2 binding. The binding characteristics were assayed using gel filtration (Figure 4A,B) and microfiltration (Figure 4C). Both assays rendered the same results; mainly data of the former are shown.

Binding to micelles of WT actophorin and of the mutants, carrying a single lysine to glutamic acid substitution, as a function of PIP_2 concentration is shown in Figure 4A. Relative to WT actophorin, PIP_2 binding of K107 was not affected and that of K105E and K94E was slightly affected. In contrast, mutations K106E and K92E lead, at the highest PIP_2 concentration that was tested, to an approximately 50 and 75% reduction in the amount of bound actophorin, respectively. These data clearly demonstrate that this α-helical region contributes to the PIP_2−actophorin interface that consequently overlaps with the actin binding surface.

PIP_2 Binding Is Enhanced by Introducing an Extra Positive Charge in the Central Part of the α-Helical Region. As both ends of the α-helical region appear to be implicated in the actophorin−PIP_2−micelle interaction, we also set out to analyze the role of charges in the middle of this secondary structural element, namely, K101 and D102. First, we compared the calculated electrostatic potential of molecules with changes at these positions with that of WT. As shown in Figure 5, the impact is fairly dramatic for mutant D102K. In WT actophorin (Figure 5, left), the regions of positive potential (blue) are relatively dispersed along the actin binding α-helical region. By in silico introduction of lysine instead of aspartic acid at position 102 in the mutant (Figure 5, right), these regions are linked together to a bulgy positive patch predicting an improvement of the attractive properties of this mutant for PIP_2 micelles relative to WT. Guided by these modeling experiments, we constructed a set of mutants. We assayed the stability (Table 1) and actin binding capacity of these mutants (Table 2). They all show a WT or nearly WT actin binding. Of particular interest is mutant D102K that appears not to be affected in its actin binding capacity. In contrast, the binding data in panels B and C of Figure 4

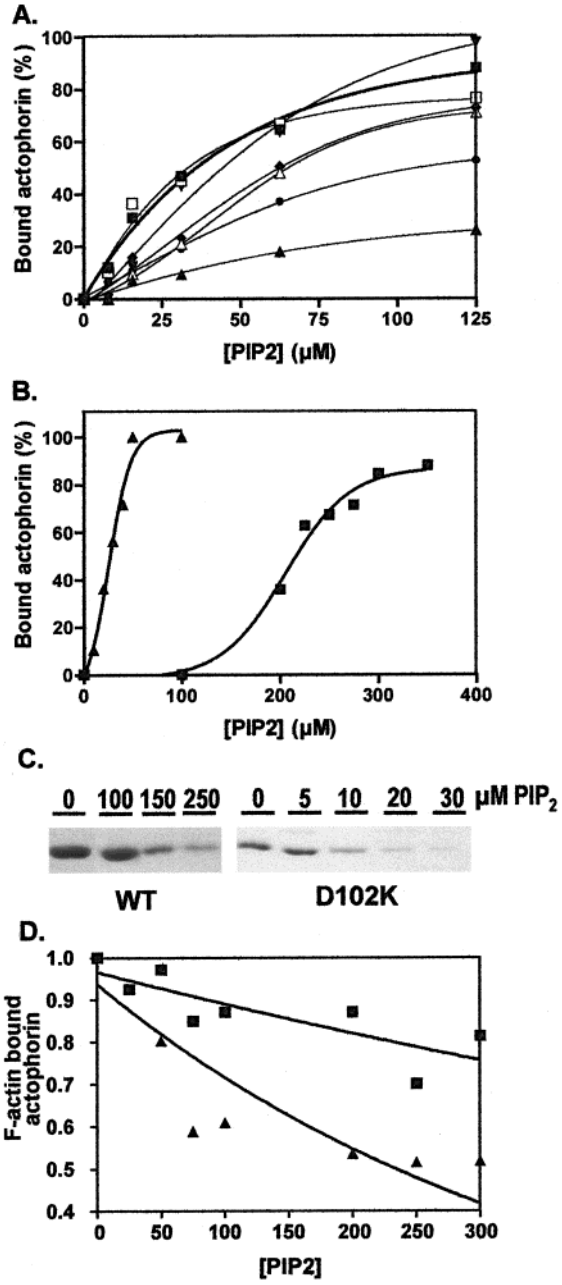

FIGURE 4: PIP_2 binding activity of actophorin WT and mutants. (A) For each data point, a gel filtration run was performed at a constant actophorin concentration of 5 μM and the indicated PIP_2 concentration. The graph shows the percentage of bound actophorin [WT (■), K92E (▲), K94E (△), K105E (◆), K106E (●), K107E (□), and KD101,102AA (▼)] as a function of PIP_2 concentration. (B) For actophorin WT (■) and D102K (▲), similar experiments were performed as described for panel A. The actophorin concentration was 20 μM. (C) SDS−PAGE analysis of the filtrates of a microfiltration experiment, containing the unbound actophorin, is shown. The actophorin WT and D102K concentration used is 5 μM, and the PIP_2 concentrations are indicated above each lane. (D) The competition between actin filaments and PIP_2 for binding actophorin WT or mutant D102K is shown. Mixtures of actophorin (15 μM), F-actin (15 μM), and PIP_2 micelles (PIP_2 concentration varying from 0 to 300 μM) were subjected to sedimentation. Pellets, containing F-actin-bound protein, were analyzed by SDS−PAGE and quantified by densitometry. The relative amount of F-actin-bound actophorin WT (■) and D102K (▲) is shown as a function of PIP_2 concentration. The amount of actophorin protein bound to F-actin in the absence of PIP_2 is set to 1.

(resulting from gel filtration and microfiltration analysis, respectively) demonstrate that mutant D102K shows a 1 order of magnitude stronger binding to PIP_2 micelles than WT. Removal of both charges in the central part of the α-helix (mutant KD101,102AA) did not affect PIP_2 binding activity (Figure 4A), indicating that K101 has no major role in binding to the negatively charged PIP_2 headgroup.

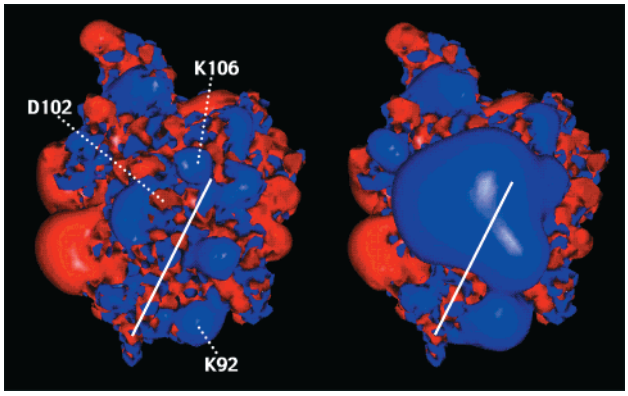

FIGURE 5: Electrostatic potential of actophorin WT and D102K. The contours of electrostatic potential for the wild type (left) and D102K mutant (right) molecule are shown (same orientation as in Figure 6). The location of the axis of the α-helical region formed by residues 91−108 is indicated by a line. Red and blue represent the negative and positive electrostatic potential, respectively. In the WT molecule, the positions of the residues that strongly affect PIP_2 binding upon substitution are indicated.

If mutant D102K exhibits an increased affinity for PIP_2, this should be reflected in an increased level of inhibition of actin binding. To test this, we incubated a constant amount of F-actin with a constant amount of WT or mutant D102K actophorin together with varying concentrations of PIP_2. Indeed, competition occurs more efficiently for D102K as less PIP_2 is required to decrease the amount of actin-bound protein (Figure 4D).

DISCUSSION

Lysine Residues in the COOH-Terminal Half of the Actin Binding α-Helical Region Contribute to F-Actin Binding. The overall degree of identity within the cofilin/ADF family is sufficiently large to assume they contact actin filaments in a very similar way (*46*). The variations, apparent from aligning primary and overlaying tertiary structures, however, suggest subtle differences in the detailed kinetic properties of the actin−ADF/cofilin interaction. The latter is supported by several studies in which different combinations of cofilin isoforms and one actin form (or vice versa) were compared (*12*, *47*−*49*). Therefore, in our effort to probe the importance of the ADF/cofilin α-helical region in establishing the F-actin contact using actophorin (or cofilin peptide mimetics), we chose to use assays (cross-linking and cosedimentation) that probed binding rather than detailed kinetics.

The binding data presented in this study extend the actin binding interface of ADF/cofilin (Figure 6) on the basis of previous reports for yeast and porcine cofilin (*35*, *36*). As in these studies, we demonstrate the active participation of the NH_2-terminal lysine residues (K92 and K94) but in addition clearly show also that the COOH-terminal lysine residues (K105, K106, and K107) in the actin binding α-helical region of actophorin contact F-actin. A contribution of the COOH-terminal part was up to now only suggested by peptide mimetics (*33*, *50*), and here we identify lysines that are important in actophorin. Lappalainen et al. (*36*) did

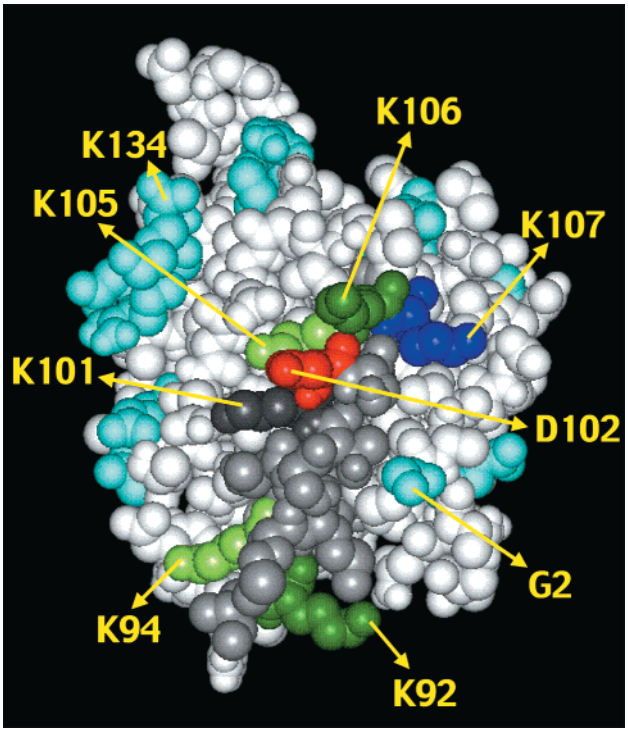

FIGURE 6: Actin- and PIP_2-interacting residues of *Acanthamoeba* actophorin. Space-filling model of actophorin (residues 2−134) (*31*) showing the location in the three-dimensional structure of the α-helical region (residues 91−108, in gray). The lysine residues within this region that are involved only in actin binding (dark blue), in actin binding and strong PIP_2 binding (dark green), or in actin binding and weak in PIP_2 binding (light green) are shown. K101, of little or no importance for both activities, is shown in dark gray; D102, resulting in a gain in the level of PIP_2 binding upon substitution into lysine, is colored in red. In cyan are shown the residues implicated in actin interaction in yeast cofilin (*23*, *36*). The first (G2) and last (K134) residue of the resolved structure indicate the approximate position of the NH_2- and COOH-termini.

not observe a significant effect on actin organization in yeast in vivo upon mutating the corresponding COOH-terminal basic residues in yeast cofilin to alanine. Whether this is due to the fact that charge reversals have more impact on actin interaction than the change from lysine to alanine or due to the use of a less sensitive in vivo assay is presently unclear. Indirect support for the participation of the COOH-terminal residues in contacting actin comes from a recent study (*14*) on the function of the central kink in the α-helical region studied here (*30*−*32*). This kink evidently influences the spatial position of the following residues, and one can argue that the functional significance attributed to this kink (*14*) is (in part) based on the fact that residues located both NH_2- and COOH-terminally of this structural irregularity need to be in a defined relative orientation for efficient complex formation.

Ca^{2+}-Dependent F-Actin Binding of Actophorin Mutants May Mimic Segment 2-Mediated F-Actin Binding by Gelsolin-Related Proteins. Intriguingly, our data suggest that the actin binding capacity of actophorin mutants carrying a charge reversal of the COOH-terminal lysines K105, K106, and K107 can be partially restored when Ca^{2+} is present. Evidently, actin binding by members of the cofilin/ADF family does not require calcium. However, the observed Ca^{2+} dependence of the COOH-terminal mutants strengthens our view that cofilin is a gelsolin segment 2 homologue (*33*), binding to a similar site on the actin filament by contacting two neighboring actin monomers (*51*−*53*). On the basis of a structural overlay, gelsolin segment 2 R221 corresponds to actophorin K105. In contrast, severin, the gelsolin analogue of *Dictyostelium*, has an acidic residue at this position in segment 2 (D182). Severin interacts with actin in a Ca^{2+}-dependent fashion (*45*). Moreover, NMR analysis of the second severin segment demonstrated that this residue complexes Ca^{2+} (*54*). The fact that the residues at the corresponding position in gelsolin segment 2 and in actophorin are basic is consistent with their Ca^{2+}-independent actin binding (*1*, *55*) and suggests that by exchanging lysine for glutamic acid in actophorin we altered the charges in the actin binding surface of actophorin, thereby mimicking the Ca^{2+}-dependent F-actin association of severin segment 2. Unfortunately, we were unable to check the Ca^{2+} dependence of a gelsolin segment 2 variant carrying a negative charge at the relevant position (221) because the mutant segment was unstable upon production in *E. coli*.

The Binding Sites of Actin and PIP_2 on Actophorin Overlap. Proteins of the ADF/cofilin family also interact with the signaling molecule PIP_2. K92 and K106 are crucial in PIP_2 binding and participate in F-actin interaction; the other lysines of the α-helical region involved in F-actin binding do not or weakly affect PIP_2 binding (Figure 6). Hence, the overlap between the actin and PIP_2 binding sites is only partial but sufficient to explain the mutually exclusive binding of these two ligands on actophorin. This shared binding site is spatially close to the actophorin extreme NH_2-terminus that has been implicated in PIP_2 and actin binding in yeast and chicken cofilin (*36*, *56*). Consequently, the overlap between the actin and PIP_2 binding sites on actophorin is likely to be even more extensive.

Mutually exclusive PIP_2 and actin binding has been described for other actin binding proteins, e.g., profilin (*57*) and gelsolin (*44*). In the case of profilin, this is also due to partially overlapping binding sites (*58*, *59*). The globally similar fold between domains of gelsolin and ADF/cofilin (*30*) allows a structural comparison of their proposed PIP_2 binding sites. Two such sites, characterized by the consensus sequence $K/R(X)_{3/4}KXK/RK/R$, have been identified in segment 2 of various gelsolin members (*60*, *61*). In the three-dimensional structure of gelsolin segment 2 (*62*), some of the basic residues in these motifs (residues 135, 168, and 169) group together at one edge of the central β-sheet close to the gelsolin segment 2 actin binding α-helix (*63*) that corresponds to the α-helical region in actophorin. Interestingly, villin residues at some of the homologous positions (corresponding to gelsolin residues 168 and 169) are also involved in F-actin binding (*64*). In this respect, it is also noteworthy that some of the positive charges on the actin binding α-helix of gelsolin segment 2 are conserved with respect to cofilin and actophorin (*29*, *33*). Thus, in addition to analogous F-actin binding (*33*), gelsolin segment 2 and cofilin may display similar PIP_2 binding and/or regulation.

Increasing the Positive Electrostatic Potential of the Actophorin α-Helix Promotes PIP_2 Binding. The observed gain in the extent of PIP_2 binding for actophorin mutant D102K probably results from the dramatic increase in the positive electrostatic potential of its α-helical region. The net positive charge of the α-helical region differs between ADF/cofilin isoforms, suggesting their affinity for PIP_2 may

vary. Also, the extent of "kinking" of the α-helical region in the different isoforms will affect the shape of the positively charged PIP_2 target surface. In cells, the strength of the PIP_2 interaction of ADF/cofilins may modulate the availability of cofilins for binding and depolymerizing actin filaments. The latter activity forms a key step in a recently suggested regulated treadmilling model of actin-based cellular motility (*65*). Thus, the delicate balance between PIP_2 and actin binding may be important in the reorganization of actin networks. As it is unaffected in actin binding but its actin binding more efficiently inhibited by PIP_2, our gain-of-function mutant will be an important tool in elucidating the regulation of ADF/cofilin action on actin by PIP_2 in vivo. Moreover, in combination with other mutations, the D102K substitution may allow us to unravel possible interactions between the PIP_2 and other regulatory pathways. Several studies have shown that cofilin is translocated to the plasma membrane upon cell stimulation and is concomitantly activated by dephosphorylation (references in ref *66*). PIP_2 could function in recruiting cofilin and/or phosphorylated cofilin to the cell periphery, presenting it to either the phosphatase or the kinase. Meberg et al. (*67*) showed that after stimulation of certain cell types the phosphate turnover on ADF is strongly enhanced whereas the net amount of activated cofilin remains unchanged, which is indicative of simultaneous but spatially separated activation and deactivation. Consequently, understanding the possible role of PIP_2 in specifically localizing cofilins will be of major interest.

ACKNOWLEDGMENT

We thank Prof. Dr. T. Pollard for providing the actophorin plasmid, Prof. Dr. M. Van Montagu for the use of the PhosphorImager, Prof. Dr. F. Van Roy for providing access to his DNA sequencing facilities, and J. Van Damme for the mass measurements on the cofilin peptides.

REFERENCES

1. Bamburg, J. R. (1999) *Annu. Rev. Cell Dev. Biol. 15*, 185−230.
2. Lappalainen, P., and Drubin, D. G. (1997) *Nature 388*, 78−82.
3. Carlier, M.-F., Ressad, F., and Pantaloni, D. (1999) *J. Biol. Chem. 274*, 33827−33830.
4. Bamburg, J. R., McGouch, A., and Ono, S. (1999) *Trends Cell Biol. 9*, 364−370.
5. Moon, A. L., Janmey, P. A., Louie, K. A., and Drubin, D. G. (1993) *J. Cell Biol. 120*, 421−435.
6. Iida, K., Moriyama, K., Matsumoto, S., Kawasaki, H., Nishida, E., and Yahara, I. (1993) *Gene 124*, 115−120.
7. Gunsalus, K. C., Bonaccorsi, S., Williams, E., Verni F., Gatti, M., and Goldberg, M. L. (1995) *J. Cell Biol. 131*, 1243−1259.
8. Abe, H., Obinata, T., Minamide, L., and Bamburg, J. R. (1996) *J. Cell Biol. 132*, 871−885.
9. Aizawa, H., Sutoh, K., and Yahara, I. (1996) *J. Cell Biol. 132*, 335−344.
10. Aizawa, H., Katadae, M., Maruya, M., Sameshima, M., Murkami-Murofushi, K., and Yahara, I. (1999) *Genes Cells 4*, 311−324.
11. Yonezawa, N., Nishida, E., and Sakai, H. (1985) *J. Biol. Chem. 260*, 14410−14412.
12. Blanchoin, L., and Pollard, T. D. (1999) *J. Biol. Chem. 274*, 15538−15546.
13. Maciver, S. K. (1998) *Curr. Opin. Cell Biol. 10*, 140−144.
14. Moriyama, K., and Yahara, I. (1999) *EMBO J. 18*, 6752−6761.
15. Carlier, M.-F., Laurent, V., Santolini, J., Melki, R., Didry, D., Xia, G.-X., Hong, Y., Chua, N.-H., and Pantaloni, D. (1997) *J. Cell Biol. 136*, 1307−1323.
16. Ressad, F., Didry, D., Egile, C., Pantaloni, D., and Carlier, M.-F. (1999) *J. Biol. Chem. 274*, 20970−20976.
17. Edwards, D. C., Sanders, L. C., Bokoch, G. M., and Gill, G. N. (1999) *Nat. Cell Biol. 1*, 253−259.
18. Maekawa, M., Ishizaki, T., Boku, S., Watanabe, N., Fujita, A., Iwamatsu, A., Obinata, T., Ohashi, K., Mizuno, K., and Narumiya, S. (1999) *Science 285*, 895−898.
19. Arber, S., Barbayannis, F. A., Hanser, H., Schneider, C., Stanyon, C. A., Bernard, O., and Caroni, P. (1998) *Nature 393*, 805−809.
20. Agnew, B. J., Minamide, L. S., and Bamburg, J. R. (1995) *J. Biol. Chem. 270*, 17582−17586.
21. Moriyama, K., Iida, K., and Yahara, I. (1996) *Genes Cells 1*, 73−86.
22. Lian, J. P., Marcks, P. G., Wang, J. Y., Falls, D. L., and Badley, J. A. (2000) *J. Biol. Chem. 275*, 2869−2876.
23. Rodal, A. A., Tetreault, J. W., Lappalainen, P., Drubin, D. G., and Amberg, D. (1999) *J. Cell Biol. 145*, 1251−1264.
24. Okada, K., Obinata, T., and Abe, H. (1999) *J. Cell Sci. 112*, 1553−1565.
25. Iida, K., and Yahara, I. (1999) *Genes Cells 4*, 21−32.
26. Yonezawa, N., Nishida, E., Iida, K., Yahara, I., and Sakai, H. (1990) *J. Biol. Chem. 265*, 8382−8386.
27. Quirck, S., Maciver, S. K., Ampe, C., Doberstein, S., Kaiser, D., Vandamme, J., Vandekerckhove, J., and Pollard, T. D. (1993) *Biochemistry 32*, 8525−8533.
28. Nagaoka, R., Kusano, K., Abe, H., and Obinata, T. (1995) *J. Cell Sci. 108*, 581−593.
29. Van Troys, M., Vandekerckhove, J., and Ampe, C. (1999) *Biochim. Biophys. Acta 1448*, 323−348.
30. Hatanaka, H., Ogura, K., Moriyama, K., Ichikawa, S., Yahara, I., and Inagaka, F. (1996) *Cell 85*, 1047−1055.
31. Leonard, S. A., Gittis, A. G., Petrella, E. C., Pollard, T. D., and Lattman, E. E. (1997) *Nat. Struct. Biol. 4*, 369−373.
32. Fedorov, A. A., Lappalainen, P., Fedorov, E. V., Drubin, D. G., and Almo, S. C. (1997) *Nat. Struct. Biol. 4*, 366−369.
33. Van Troys, M., Dewitte, D., Verschelde, J.-L., Goethals, M., Vandekerckhove, J., and Ampe, C. (1997) *J. Biol. Chem. 272*, 32750−32758.
34. Cooper, J. A., Blum, J. D., Williams, R. C., Jr., and Pollard, T. D. (1986) *J. Biol. Chem. 261*, 477−485.
35. Moriyama, K., Yonezawa, N., Sakai, H., Yahara, I., and Nishida, E. (1992) *J. Biol. Chem. 267*, 7240−7244.
36. Lappalainen, P., Fedorov, E. V., Fedorov, A. A., Almo, S. C., and Drubin, D. G. (1997) *EMBO J. 16*, 5520−5530.
37. Van Troys, M., Dewitte, D., Goethals, M., Carlier, M.-F., Vandekerckhove, J., and Ampe, C. (1996) *EMBO J. 15*, 201−210.
38. Sasagawa, T., Titani, K., and Walsch, K. A. (1983) *Anal. Biochem. 128*, 371−376.
39. Vancompernolle, K., Goethals, M., Huet, C., Louvard, D., and Vandekerckhove, J. (1992) *EMBO J. 11*, 4739−4746.
40. Spudich, J. A., and Watt, S. (1971) *J. Biol. Chem. 246*, 4866−4871.
41. Kouyama, T., and Michashi, K. (1981) *Eur. J. Biochem. 114*, 33−38.
42. Ho, S. N., Hunt, H. D., Horton, R. M., Pullen, J. K., and Pease, L. R. (1989) *Gene 77*, 51−59.
43. Lambrechts, A., Verschelde, J.-L., Jonckheere, V., Goethals, M., Vandekerckhove, J., and Ampe, C. (1997) *EMBO J. 16*, 484−494.
44. Yin, H. L., Iida, K., and Janmey, P. A. (1988) *J. Cell Biol. 106*, 805−812.
45. Eichinger, L., and Schleicher, M. (1992) *Biochemistry 31*, 4779−4787.
46. Lappalainen, P., Kessels, M. M., Cope, M. J., and Drubin, D. G. (1998) *Mol. Biol. Cell 9*, 1951−1959.
47. Ono, S., and Benian, G. M. (1998) *J. Biol. Chem. 273*, 3778−3783.
48. Maciver, S. K., Pope, B. J., Whytock, S., and Weeds, A. G. (1998) *Eur. J. Biochem. 256*, 388−397.

49. Ono, S. (1999) *Cell Motil. Cytoskeleton 43*, 128−136.
50. Yonezawa, N., Nishida, E., Ohba, M., Seki, M., Kumagai, H., and Sakai, H. (1989) *Eur. J. Biochem. 183*, 235−238.
51. McGouch, A., and Way, M. (1995) *J. Struct. Biol. 115*, 144−150.
52. McGouch, A., Pope, B., Chui, W., and Weeds, A. (1997) *J. Cell Biol. 138*, 771−781.
53. Renoult, C., Ternent, D., Maciver, S. K., Fattoum, A., Astier, C., Benyamin, Y., and Roustan, C. (1999) *J. Biol. Chem. 274*, 28893−28899.
54. Schnuchel, A., Wiltscheck, R., Eichinger, L., Schleicher, M., and Holak, T. (1995) *J. Mol. Biol. 247*, 21−27.
55. Way, M., Gooch, J., Pope, B., and Weeds, A. G. (1989) *J. Cell Biol. 109*, 593−605.
56. Kusano, K., Abe, H., and Obinata, T. (1999) *Mol. Cell. Biochem. 190*, 133−141.
57. Lassing, I., and Lindberg, U. (1985) *Nature 314*, 472−474.
58. Fedorov, A. A., Magnus, K. A., Graupe, M. H., Lattman, E. E., Pollard, T. D., and Almo, S. C. (1994) *Proc. Natl. Acad. Sci. U.S.A. 91*, 8636−8640.
59. Sohn, R., Chen, J., Kobland, K., Bray, P., and Goldschmidt-Clermont, P. (1995) *J. Biol. Chem. 270*, 21114−21120.
60. Yu, F.-X., Sun, H.-Q., Janmey, P. A., and Yin, H. L. (1992) *J. Biol. Chem. 267*, 14616−14621.
61. Kwiatkowski, D. J., Janmey, P. A., and Yin, H. L. (1989) *J. Cell Biol. 108*, 1717−1726.
62. Burtnick, L. D., Koepf, E. K., Grimes, J., Jones, E. Y., Stuart, D. I., McLaughlin, P. J., and Robinson, R. C. (1997) *Cell 90*, 661−670.
63. Van Troys, M., Dewitte, D., Goethals, M., Vandekerckhove, J., and Ampe, C. (1996) *FEBS Lett. 397*, 191−196.
64. Friederich, E., Vancompernolle, K., Louvard, D., and Vandekerckhove, J. (1999) *J. Biol. Chem. 274*, 26751−26760.
65. Machesky, L. M., and Insall, R. H. (1999) *J. Cell Biol. 146*, 267−272.
66. Yahara, I., Aizawa, H., Moriyama, K., Iida, K., Yonezawa, N., Nishida, E., Hatanaka, H., and Inagaki, F. (1996) *Cell Struct. Funct. 21*, 421−424.
67. Meberg, P. J., Ono, S., Minamide, L. S., Tahahashi, M., and Bamburg, J. R. (1998) *Cell Motil. Cytoskeleton 39*, 172−190.

BI000816C